NIH Public Access
Author Manuscript
Cytometry A. Author manuscript; available in PMC 2010 December 1.

Published in final edited form as:
Cytometry A. 2009 December ; 75(12): 1031–1039. doi:10.1002/cyto.a.20790.

Green fiber lasers: An alternative to traditional DPSS green lasers for flow cytometry

William G. Telford[1,*], **Sergey A. Babin**[2,§], **Serge V. Khorev**[2], and **Stephen H. Rowe**[2]
[1]Experimental Transplantation and Immunology Branch, NCI-NIH, Bethesda, MD, USA
[2]Zecotek Laser Systems Pte. Ltd., Zecotek Photonics Inc., Singapore

Abstract

Green and yellow diode-pumped solid state (DPSS) lasers (532 and 561 nm) have become common fixtures on flow cytometers, due to their efficient excitation of phycoerythrin (PE) and its tandems, and their ability to excite an expanding array of expressible red fluorescent proteins. Nevertheless, they have some disadvantages. DPSS 532 nm lasers emit very close to the fluorescein bandwidth, necessitating optical modifications to permit detection of fluorescein and GFP. DPSS 561 nm lasers likewise emit very close to the PE detection bandwidth, and also cause unwanted excitation of APC and its tandems, requiring high levels of crossbeam compensation to reduce spectral overlap into the PE tandems. In this paper, we report the development of a new generation of green fiber lasers that can be engineered to emit in the range between 532 and 561 nm. A 550 nm green fiber laser was integrated into both a BD LSR II™ cuvette and FACSVantage DiVa™ jet-in-air cell sorter. This laser wavelength avoided both the fluorescein and PE bandwidths, and provided better excitation of PE and the red fluorescent proteins DsRed and dTomato than a power-matched 532 nm source. Excitation at 550 nm also caused less incidental excitation of APC and its tandems, reducing the need for crossbeam compensation. Excitation in the 550 nm range therefore proved to be a good compromise between 532 and 561 nm sources. Fiber laser technology is therefore providing the flexibility necessary for precisely matching laser wavelengths to our flow cytometry applications.

Keywords

Flow cytometry; fiber laser; phycoerythrin; red fluorescent protein; DsRed

Introduction

Flow cytometry relies almost exclusively on lasers as sources of excitation for fluorescent probes. While their coherence and power level makes them ideal tools for illuminating individual cells, they have traditionally provided a limited range of excitation wavelengths. Nevertheless, recent advances in solid state laser technology have vastly increased the number of wavelengths available for flow cytometric analysis (1-4). A good example of this is the recent trend toward the incorporation of green and yellow laser sources into flow cytometers. Diode-pumped solid state (DPSS) 532 nm green lasers are now common fixtures on modern flow cytometers (5). These lasers are mainly used to replace the traditional 488 nm excitation of phycoerythrin (PE) and its tandems. While 488 nm laser

*To whom correspondence should be addressed: William Telford, National Cancer Institute, Building 10 Room 3-3297, 9000 Rockville Pike, Bethesda, MD 20892 USA. Phone: 301-435-6379. telfordw@mail.nih.gov.
§Permanent address: Institute of Automation and Electrometry, Siberian Branch of Russian Academy of Sciences, Novosibirsk 630090, Russia

NIH-PA Author Manuscript
NIH-PA Author Manuscript
NIH-PA Author Manuscript

NIH-PA Author Manuscript

NIH-PA Author Manuscript

NIH-PA Author Manuscript

sources have traditionally been used to excite both fluorescein and PE for multicolor flow cytometry, this wavelength does not provide optimal excitation of PE, acting instead on a minor shoulder in the PE excitation spectrum. Green 532 nm laser light emits closer to the excitation maximum for PE, resulting in substantially improved signal-to-background ratios and detection sensitivity for PE, and in particular the PE tandem conjugates. Green lasers also excite less cellular autofluorescence, further improving fluorochrome sensitivity. Finally, green lasers provide substantially better excitation of the shorter wavelength red fluorescent proteins than traditional 488 nm sources, including DsRed and dTomato, and can excite other useful probes like the rhodamine derivatives (6,7). However, 532 nm laser light coincides closely with the fluorescein emission bandwidth; if fluorescein is to be detected on a cytometer equipped with a 532 nm laser, the traditional 530/30 nm fluorescein bandpass filter must be replaced with a shorter wavelength filter (usually a 510/20 nm or similar) that is strongly blocked for 532 nm laser light. This modification can reduce fluorescein sensitivity, and 532 nm laser light spillover into the fluorescein detector can still occur even with these optical modifications.

More recently, DPSS 561 nm laser sources have become commercially available at relatively high power levels. The 561 nm wavelength coincides almost precisely with the excitation maximum for PE, and can also replace the traditional 488 nm laser for PE excitation (8). The 561 nm laser also emits further from the fluorescein emission bandwidth than 532 nm sources, eliminating the need for modifying the fluorescein filters when integrating the laser. As with the green, 561 nm sources also excite less cellular autofluorescence, similarly improving signal detection by reducing background fluorescence. Green-yellow 561 nm laser light also provides excellent excitation of the mid-range red fluorescent proteins, including mCherry and mStrawberry (6,7,8). However, 561 nm lasers are also not completely ideal for multicolor analysis. This laser wavelength is close to the emission bandwidth for phycoerythrin; 561 nm light impinges on the transmission ranges for the 575/25 and 585/42 nm bandpass filters traditionally used for PE detection. Using a 561 nm laser for PE and PE tandem excitation requires modifying the range of the PE bandpass filter to a minimum of 590/20 nm, resulting in a small loss of PE sensitivity. Green-yellow 561 nm laser light also overlaps the excitation curve of allophycocyanin (APC), another immunophenotyping label that is frequently combined with fluorescein, PE and PE tandem dyes for multicolor immunolabeling. While not as optimal as a red laser, the 561 nm laser can excite APC to a considerable extent; in cells simultaneously labeled with the PE tandem conjugate PE-Cy5, this can cause unwanted fluorescence spillover into the PE-Cy5 detector, which requires a bandpass filter similar to that used for APC. This excitation artifact requires crossbeam compensation and introduces an undesirable complication into multicolor analysis. The 561 nm excitation of APC tandems APC-Cy5.5 and APC-Cy7 causes similar problems with detection of the tandem dyes PE-Cy5.5 and PE-Cy7.

Until recently, cytometrists usually had to make the difficult choice between 532 and 561 nm sources on their instruments, since the number of laser intercepts available on commercial instruments has been small. The 532 nm laser has been more widely used and was probably the better choice when improved PE tandem excitation was the main concern, since it does not appreciably excite APC. The 561 nm was recommended when both PE tandem and excitation of long red fluorescent proteins such as mCherry was required, with the disadvantage of incidental APC excitation. Both choices involved some compromise, since neither was ideal when detecting in the fluorescein and PE emission bandwidths.

A better solution to providing more optimal PE signal detection with lower incidental APC excitation would be a laser wavelength between 532 and 561 nm. A laser in the 540 to 555 nm range would provide optimal excitation of PE, while avoiding both the fluorescein and

NIH-PA Author Manuscript

NIH-PA Author Manuscript

NIH-PA Author Manuscript

PE emission bandwidth. It would also cause reduced excitation of APC in the PE-Cy5 detection range. However, very few options exist for lasers in this emission range. Green HeNe lasers, while available in this range at 543 nm, emit at very low power levels (2 mW) and have seen limited use in flow cytometry. While a few solid state sources in the 540 to 555 nm range have been built, they have noise levels too high for flow cytometry. Lack of a good fluorescence-based biomedical application has also not encouraged technology development in this wavelength range.

In this paper, we report the development of a new class of fiber lasers that can be engineered to emit at discrete wavelengths between 515 and 560 nm. A 550 nm green fiber laser has been built that has performance properties suitable for flow cytometry, and was extensively evaluated in both cuvette and jet-in-air flow cytometers. This laser avoided both the fluorescein and PE emission bandwidths, while providing excellent excitation of PE and its tandems and the red fluorescent proteins. We propose this laser technology as a novel alternative to traditional 532 and 561 nm DPSS sources.

Materials and Methods

Cells and immunophenotyping

EL4 cells were obtained from the ATCC (Manassas, VA) and maintained in RPMI containing 10% FBS. Cells were labeled with biotin-conjugated anti-mouse CD3, CD44 or CD95 primary antibody, and secondary labeled with streptavidin conjugated to phycoerythrin (PE), PE-Cy7, allophycocyanin (APC) or APC-Cy7. All immunolabeling reagents were obtained from Invitrogen Corporation (Carlsbad, CA). pDsRed1-1 and ptdTomato plasmids were inserted into a murine stem cell virus (MSCV) Neo^r vector backbone and transduced into SP2/0 cells followed by G418 selection (9).

Lasers and flow cytometry

The following laser sources were used in this study: (i) A green fiber laser (Zecotek Laser Systems, Singapore) emitting at 550 nm, with a variable power output of 50 to 150 mW and a RMS noise level of less than 1% (Figure 1a-c) in single mode TEM_{00} with a beam diameter of approximately 0.6 mm with good coherence; (ii) a DPSS 532 nm laser (Laser-Compact, Moscow, Russia) with a fixed power output of 50 mW, RMS noise less than 1% in single mode TEM_{00}; (iii) a DPSS 532 nm laser (Oxxius, France) with a fixed power output of 150 mW, RMS noise less than 0.5% in single mode TEM_{00}; (iv) a DPSS 561 nm laser (Oxxius, France) with a fixed power output of 50 mW, RMS noise less than 0.5% in single mode TEM_{00}. Laser beam profiles were modified using a 3× beam expander (CVI Melles Griot, Carlsbad, CA), and beam profiles measured using a DataRay CCD camera (DataRay, Boulder Creek, CA). The resulting beam profiles for all evaluated lasers were normalized to a Gaussian distribution with a 50% beam waist diameter of approximately 0.8 millimeters at a position immediately prior to the LSR II laser focusing lens (10). All laser power levels were monitored using a power meter with semiconductor detector (Thorlabs, Newton, NJ). All lasers were mounted on a BD LSR II™ flow cytometer, and aligned to the PMT detector cluster normally reserved for a default HeNe red laser source. The same lasers were also mounted on a BD FACSVantage DiVa™ and aligned to the second laser position normally reserved for the red laser.

The microsphere mixtures used in this study are summarized in Table 1. Instrument alignment for all lasers was optimized using premixed Spherotech Rainbow 8-population microspheres (Spherotech, Lake Forest, IL). All microsphere mixtures, PE labeled and DsRed and dTomato expressing cells were analyzed using the following bandpass filters: 585/42 nm (Omega Optical, Brattleboro, VT) and 585/40 nm, 575/25 nm, 585/40 nm and

NIH-PA Author Manuscript

NIH-PA Author Manuscript

NIH-PA Author Manuscript

590/20 nm (Semrock, Rochester, NY). The same filter sets were used for both BD LSR II™ and FACSVantage DiVa™ analysis. APC labeled cells were analyzed with either 660/20 or 675/20 nm bandpass filters as indicated; APC-Cy7 labeled samples with a 780/60 nm bandpass. For crossbeam laser light contamination experiments, standard fluorescein and PE filters (510/20 nm, 530/30 nm, 585/42 nm and 590/20 nm) were used in the 488 nm aligned fluorescein and PE detectors. Non-premixed MESF FITC low intensity and non pre-mixed MESF PE low microspheres (Bangs Laboratories/Polysciences, Warrington, PA) were used to assess laser light contamination of the fluorescein and PE detectors (Table 1 and Figure 1). MESF PE microspheres were also used to determine the minimum PE bandpass filter for direct analysis (Figure 2). For all presented experiments, PMT voltages were kept at fixed values for microspheres or cells, regardless of the laser wavelength used. Maximum PMT sensitivity and linearity ranges were established according to the procedure described by Joseph Trotter at BD Biosciences (http://www.bdbiosciences.com/pdfs/whitePapers/23-8389-00.pdf) using 488 and 633 nm lasers. Briefly, the mean fluorescence intensity and C.V. for a fluorescent microsphere was measured at increasing PMT gains, and the overall distributions were plotted to determine the PMT setting showing maximum fluorescence sensitivity, linearity and resolution for each detector. These PMT voltages were fixed and used for measurements at all laser wavelengths.

Data analysis

Data were acquired using the DiVa™ acquisition software system (BD Biosciences), exported as FCS 3.0 files and analyzed using FlowJo for PC ver. 7.2.5 on a five log scale (Tree Star Software, Ashland, OR). Data was initially expressed as median log fluorescence intensity (abbreviated median) values for both the labeled and unlabeled cell populations (henceforth designated Signal and Background, respectively). The following sensitivity metric was then used to estimate signal detection over background (10,11,12):

$$\mathrm{SI}=\frac{(\text{median signal} - \text{median background})}{[(84^{\text{th}}\text{percentile median background} - \text{median background})/0.995]}$$

All values in this equation were calculated using FlowJo. The denominator of this equation is one method for calculating robust standard deviation (SD). Unlike other methods which calculate robust SD by multiplying robust CV by the median, this method weighs the right-hand slope (above the axis) of the background peak more heavily, and is therefore less affected by cells on the extremely low end of the scale. This sensitivity index therefore attempts to minimize the relatively large error associated with background fluorescence distribution, particularly when many events are at the lowest point of the axis. This sensitivity metric value is indicated on all histograms. For the PE-Cy5 - %APC spillover experiments using 532, 550 and 561 nm laser sources, compensation was calculated using both DiVa and FlowJo automated compensation algorithms.

Results and Discussion

A novel 550 nm green fiber laser using an infrared pump laser diode (976 nm) and a coupled fiber optic cavity was used in this study. An intra-cavity frequency doubling scheme allowed increased efficiency of the green light generation around 550 nm using a conventional KTP nonlinear crystal (13). All optical elements for this laser were contained were a single grounded casing, with a power supply connected by a single umbilical cable. The resulting unit could therefore be readily mounted on both a BD LSR II™ cuvette cytometer and a BD FACSVantage DiVa™ cell sorter. For the LSR II™, the laser beam was aligned into the

NIH-PA Author Manuscript

NIH-PA Author Manuscript

NIH-PA Author Manuscript

laser path normally reserved for the red laser source; a 520 LP dichroic was used to merge the beam with the standard 488 nm. For the FACSVantage DiVa™, the laser was also aligned into the laser path normally used for the red HeNe source, and focused into the secondary signal path (of three intercepts total).

Alignment and detector sensitivity for this laser on the LSR II was then assessed using premixed Spherotech Rainbow 8-peak microspheres. The 550 nm unit was tested at three power levels (50, 100 and 150 mW), and compared to a previously evaluated 561 nm unit at 50 mW. The 550 nm unit was able to resolve all eight microsphere populations, including the dimmest population from the “unstained” control (data now shown). Both the dim bead resolution and peak C.V.s were comparable to a previously standardized 561 nm unit, indicating that the laser was properly aligned and could resolve a low-sensitivity microsphere standard.

Green 532 nm and yellow 561 nm lasers are prone to laser light impingement on standard fluorescein and PE bandpass filters respectively, forcing modification of detection optics and potentially reducing detection sensitivity. The 550 nm laser was therefore tested for its incidental contamination of the spatially separated fluorescein and PE detectors equipped with conventional narrow bandpass filters (530/30 nm and 585/42 nm). When MESF FITC low fluorescence microspheres were analyzed in the 488 nm-aligned fluorescein channel with 532, 550 or 561 nm power-matched laser simultaneously aligned to a different detection pinhole, the 532 nm showed considerable overlap into a standard 530/30 nm bandwidth filter, elevating the fluorescence background and preventing discrimination of all but the brightest microspheres (Figure 1, second column, indicated with a black arrow). Modification of the standard fluorescein filter to a 510/20 nm was required to exclude 532 nm laser light, slightly reducing fluorescein sensitivity (Figure 1, left-most column). Similarly, the 561 nm laser could not be used with a standard 585/42 nm PE filter; the two dimmest populations of MESF PE low microspheres could not be resolved, requiring instead a 590/20 nm filter (Figure 3, right-most two columns, black arrow). This 585/42 nm filter is typical of those supplied with commercial systems, and did not exclude 561 nm laser light. However, the 550 nm laser fell neatly within these ranges, causing no loss of sensitivity or resolution of either MESF FITC or PE microspheres with any of the filters tested.

The 550 nm laser also permitted the use of more optimal bandpass filters for the direct detection of PE. With 561 nm lasers, the traditional 575 and 585 nm bandpass filters are not usable due to bandwidth overlap with the laser (8). This is shown dramatically in Figure 2, where excitation of MESF PE low fluorescence microspheres with the 561 nm laser showed very high background fluorescence with 575/25 nm and 585/40 nm filters, completely obliterating resolution of all bead populations (Figure 3, right histograms). This occurred even when using Semrock filters with unusually sharp transmission edges. A 590/20 nm filter was required with the 561 nm laser to detect PE. In contrast, the 550 nm laser produced considerably lower background on the detection bandwidths of any of the Semrock filters, demonstrating compatibility with filters more optimal for PE detection. However, even the 550 nm laser required the longest 590 nm bandpass filter to completely eliminate laser light emission into the PE detection filter when used in the direct signal path.

The ability of the 550 nm laser to excite PE and a series of red fluorescent proteins was then assessed. To compare 532, 550 and 561 nm lasers for fluorochrome excitation, real cells were used rather than microspheres, to take the effects of cellular autofluorescence into account. EL4 mouse lymphoma cells labeled with PE-conjugated anti-CD3, CD44 and CD95 were analyzed using power-matched 532, 550 and 561 nm lasers using the same optical path and filters (a 590/20 nm in this case, to accommodate the 561 nm laser). CD3, CD44 and CD95 were used as cell surface markers with low, high and intermediate cell

NIH-PA Author Manuscript

NIH-PA Author Manuscript

NIH-PA Author Manuscript

surface expression respectively. The results are shown in Figure 3 (left three columns). Both the 550 and 561 nm units gave improved PE detection compared to the 532 nm laser, and the 550 nm laser showed excitation nearly as good as the 561 nm. The 550 nm laser also showed improved excitation of DsRed and dTomato expressing cells when compared to the 532 nm, although again not quite as good as the 561 nm (Figure 3, right two columns).

Nevertheless, the 550 nm laser seemed to be a good compromise between the 532 and 561 nm units, maintaining most of the improvement of fluorochrome excitation seen with the 561 nm laser while avoiding overlap into the optimal PE bandwidth. This also held true when the 532 and 550 nm units were compared for PE, DsRed and dTomato detection using a 585/40 nm filter more optimal for PE (Figure 4). Sensitivity for PE improved by at least 1.5 fold with the 550 nm laser, and sensitivity for DsRed and dTomato nearly three-fold. This improvement with 550 nm excitation occurred even though the 585/40 nm detection filter used here probably admitted a small amount of 550 nm light (see Figure 2). Increasing the power levels of the 532 and 550 nm lasers to 150 mW caused a decline in the signal-to-background ratio of PE for both lasers, but improved DsRed and dTomato sensitivity significantly (Figure 4).

The high power levels achievable with this 550 nm laser also made it possible to integrate it into a jet-in-air cell sorting system. The laser was installed on a FACSVantage DiVa™ system, and aligned to the stream in the secondary position normally assigned to a red laser source. The unit was then tested at 50, 100 and 150 mW, in comparison with a 532 nm laser at 150 mW. Sensitivity index data from PE-labeled and DsRed and dTomato expressing cells are shown in Table 2. As with the cuvette systems, 550 nm laser light showed somewhat better PE excitation at equivalent power levels, and high laser power levels yielded diminishing returns for signal-to-background ratios for PE. Fluorescent proteins, however, gave increased sensitivity with higher power levels, with 550 nm excitation giving improved detection over 532 nm.

A significant issue when moving from 532 to 561 nm excitation of PE is increased incidental excitation of allophycocyanin (APC), a common fluorochrome in multicolor labeling protocols. Incidental excitation of APC by the 561 nm can cause a significant overlap of signal into the PE-Cy5 detector, due to the coincidence of the bandpass filter for APC and PE-Cy5. This requires significant crossbeam compensation to subtract APC fluorescence from the PE-Cy5 signal, a complication when analyzing complex multicolor labeling schemes. Likewise, incidental excitation of the tandem dyes APC-Cy5.5 and APC-Cy7 would similarly overlap into the PE-Cy5.5 and PE-Cy7 detectors respectively. Since green 532 nm laser excitation causes much less incidental excitation of APC, it is likely that 550 nm excitation would also cause less APC excitation than 561 nm, and reduce the need for PE-Cy5 minus APC crossbeam compensation. To demonstrate this, a BD LSR II™ was reconfigured as shown in Figure 5a. One detector cluster was configured to detect PE, PE-Cy5 and PE-Cy7, and aligned to either 532, 550 or 561 nm lasers. A second detector cluster was configured to detect APC, APC-Cy5.5 and APC-Cy7, and aligned to a spatially separated red HeNe laser. Cells labeled with APC and APC-Cy7 were analyzed on this system, and their signal strength and spectral overlap into the PE and PE-Cy7 detectors measured.

APC signal strength in the PE-Cy5 detector using 532, 550 and 561 nm lasers is shown in Figure 5b. The 532 nm laser showed roughly 15% excitation of APC compared to the conventional red laser; APC excitation with 550 and 561 nm sources were higher, at roughly 40 and 60% respectively (Figure 5b). The spillover of 532, 550 or 561 nm excited APC into the PE-Cy5 detector was then measured using single color APC labeled cell samples, and the spillover matrix automatically calculated using FlowJo (Figure 6). As expected, the 532

NIH-PA Author Manuscript

NIH-PA Author Manuscript

NIH-PA Author Manuscript

nm laser produced the lowest overlap of APC into the PE-Cy5 detector at 36.8%. The subtracted signal for the 561 nm laser was greater than 90%, nearly three times the 532 nm value. However, the spillover value for the 550 nm was less than twice that of the 532 nm at 62.2%. When APC-Cy7 spillover into the PE-Cy7 detector was measured, the 561 nm value was more than four times the 532 nm, but the 550 nm was less than three times greater (Figure 6). The 550 nm source was therefore a reasonable compromise between the 532 and 561 nm sources, reducing the need for crossbeam compensation in complex labeling protocols while still maintaining a reasonable level of fluorochrome sensitivity.

In summary, a 550 nm laser source intermediate in wavelength between the usual 532 and 561 nm solid state sources provided a number of advantages for flow cytometry over the traditional units. The 550 nm emission avoided both the fluorescein bandwith impinged upon by 532 nm lasers and the PE bandwidth near the 561 nm source. This eliminated the need for special optical modifications to the instrument, and avoided the risk of elevated background signal in these detectors. In addition, 550 nm excitation showed improved signal-to-background ratio for detecting PE and the fluorescent proteins DsRed and dTomato, with levels of sensitivity approaching those observed with 561 nm excitation. The shorter wavelength 550 nm source also reduced the need for crossbeam compensation associated with incidental excitation of APC and its tandems. An intermediate wavelength laser between 532 and 561 nm therefore has significant advantages when a green-to-yellow laser source is required to increase PE sensitivity, or accommodate red fluorescent proteins. As with all new laser technology, cost is still a factor in implementing this wavelength for flow cytometry; the cost of a 550 nm laser is currently 2-3 fold that of a power-equivalent 532 or 561 nm source, and commercial availability is still limited. However, improvements in fiber laser technology have made the manufacture of lasers at any wavelength in the green to orange range possible, and both cost and availability should improve in the near future. This engineering flexibility will support the goal of eliminating laser wavelength limitations for flow cytometry.

Acknowledgments

The authors wish to acknowledge Veena Kapoor and Nga Tu Voong in the NCI ETIB Flow Cytometry Laboratory for excellent technical assistance, Ashvin Abraham and Faouzi Zerrouk of Zecotek and Nicolas Feat of Oxxius Laser (France) for valuable technical advice regarding DPSS and fiber laser sources, and Dmitry Churkin of Novolaser (Novosibirsk) for technical support. We also wish to acknowledge Mario Roederer, David Parks and Marty Bigos for advice on sensitivity metrics. Teresa Hawley and Robert Hawley of the George Washington School of Medicine generously provided the DsRed and dTomato SP2/0 transfectants. This work was supported by intramural research funds provided by the Center for Cancer Research, National Cancer Institute, National Institutes of Health.

Literature Cited

1. Telford, WG. Small lasers in flow cytometry. In: Hawley, TS.; Hawley, RG., editors. Methods in Molecular Biology. 2nd. Vol. 263. Humana Press; London, UK: 2004. p. 399-418.Flow Cytometry Protocols
2. Telford WG, Huber C. Novel solid-state lasers in flow cytometry. Biophotonics Intl. 2006; 13:50–53.
3. Nakamura, S.; Fasol, G. GaN based light emitters and lasers. Berlin: Springer; 1997. The blue laser diode.
4. Shapiro HM, Perlmutter NG. Violet laser diodes as light sources for cytometry. Cytometry. 2001; 44:133–136. [PubMed: 11378864]
5. Perfetto SP, Roederer M. Increased immunofluorescence sensitivity using 532 nm excitation. Cytometry A. 2007; 71A:73–79. [PubMed: 17200955]
6. Chudakov DM, Lukyanov S, Lukyanov KA. Fluorescent proteins as a toolkit for in vivo imaging. Trends Biotechnol. 2005; 23:605–613. [PubMed: 16269193]

NIH-PA Author Manuscript

NIH-PA Author Manuscript

NIH-PA Author Manuscript

7. Shaner NC, Campbell RE, Steinbach PA, Giepmans BNG, Palmer AE, Tsien RY. Improved monomeric red, orange and yellow fluorescent proteins derived from Discosoma sp. red fluorescent proteins. Nature Biotechnol. 2004; 22:1567–1572. [PubMed: 15558047]
8. Telford WG, Murga M, Hawley T, Hawley RG, Packard BZ, Komoriya A, Haas F, Hubert C. DPSS yellow-green 561 nm lasers for improved fluorochrome detection by flow cytometry. Cytometry A. 2005; 68A:36–44. [PubMed: 16163703]
9. Hawley TS, Telford WG, Ramezani A, Hawley RG. “Rainbow” reporters for multispectral marking and lineage analysis of hematopoietic stem cells. Stem Cells. 2001; 19:118–124. [PubMed: 11239166]
10. Kapoor V, Karpov V, Linton C, Subach FV, Verkhusha VV, Telford WG. Solid state yellow and orange lasers for flow cytometry. Cytometry A. 2008; 73A:570–577. [PubMed: 18449918]
11. Chase ES, Hoffman RA. Resolution of dimly labeled particles: a practical measure of fluorescent sensitivity. Cytometry. 1998; 33:267–279. [PubMed: 9773890]
12. Bigos, M. Separation index: An easy-to-use metric for evaluation of different configurations on the same flow cytometer. In: Robinson, JP., et al., editors. Current Protocols in Cytometry. New York, NY: John Wiley and Sons; 2007. p. 1.21.1-1.21.6.
13. Akulov VA, Afanasiev DM, Babin SA, Churkin DV, Kablukov SI, Rybakov MA, Vlasov AA. Frequency tuning and doubling in Yb-doped fiber lasers. Laser Phys. 2007; 17:124–129.

Abbreviations

DPSS	diode-pumped solid state
R-PE	R-phycoerythrin

NIH-PA Author Manuscript

NIH-PA Author Manuscript

NIH-PA Author Manuscript

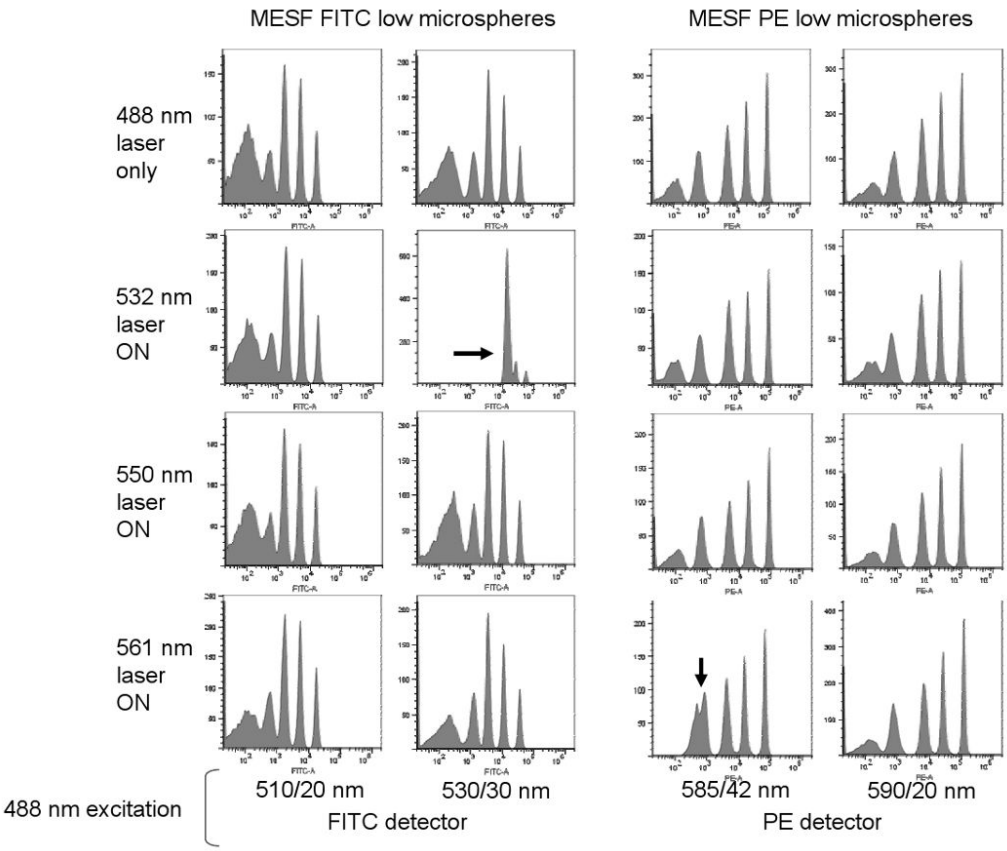

Figure 1. Laser light contamination of fluorescein and PE detectors

532, 550 or 561 nm lasers were mounted and aligned on a BD LSR II™, and MESF FITC low microspheres (left two columns) and MESF PE low microspheres (right two columns) were subsequently analyzed in the 488 nm aligned fluorescein and PE detectors respectively (spatially separated from the 532, 550 or 561 nm optical path). A 510/20 nm or 530/30 nm filter was used for MESF FITC microsphere detection, and a 585/42 or 590/20 nm filter for MESF PE microsphere detection. Loss of dim microsphere resolution is marked with black arrows.

NIH-PA Author Manuscript

NIH-PA Author Manuscript

NIH-PA Author Manuscript

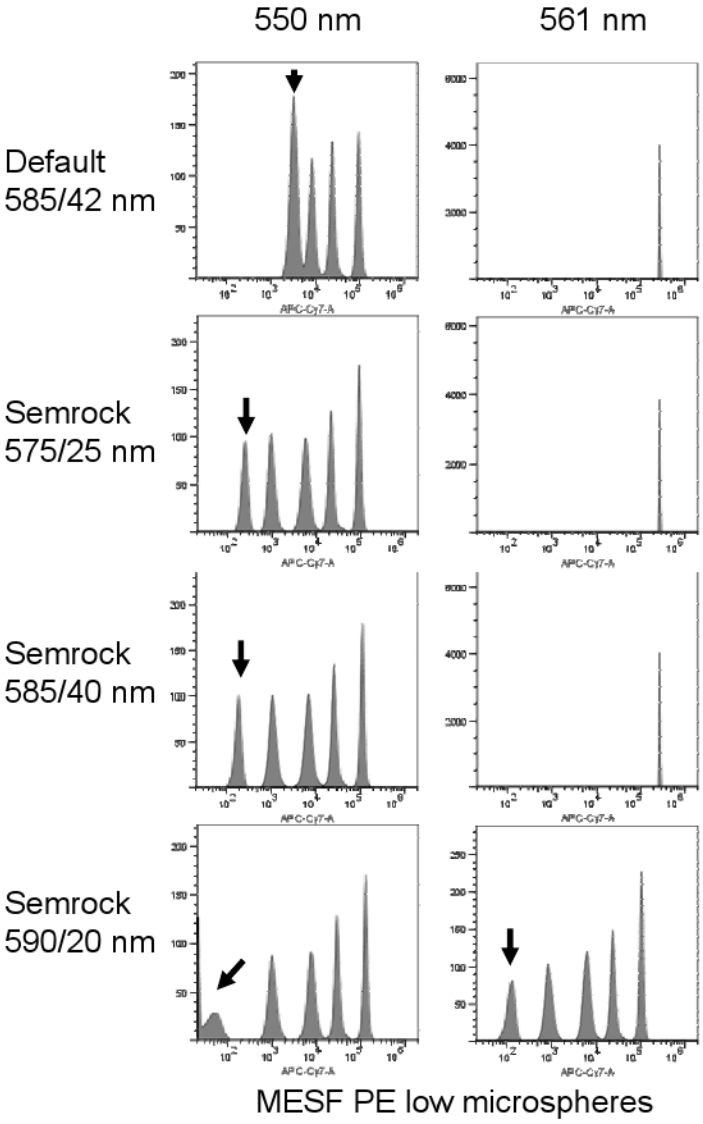

Figure 2. Appropriate PE filter for 550 nm laser excitation

550 or 561 nm lasers were mounted and aligned on a BD LSR II™, and non-premixed MESF PE microspheres were analyzed using the indicated bandpass filters. Black arrows indicate the location of the dimmest bead population.

NIH-PA Author Manuscript

NIH-PA Author Manuscript

NIH-PA Author Manuscript

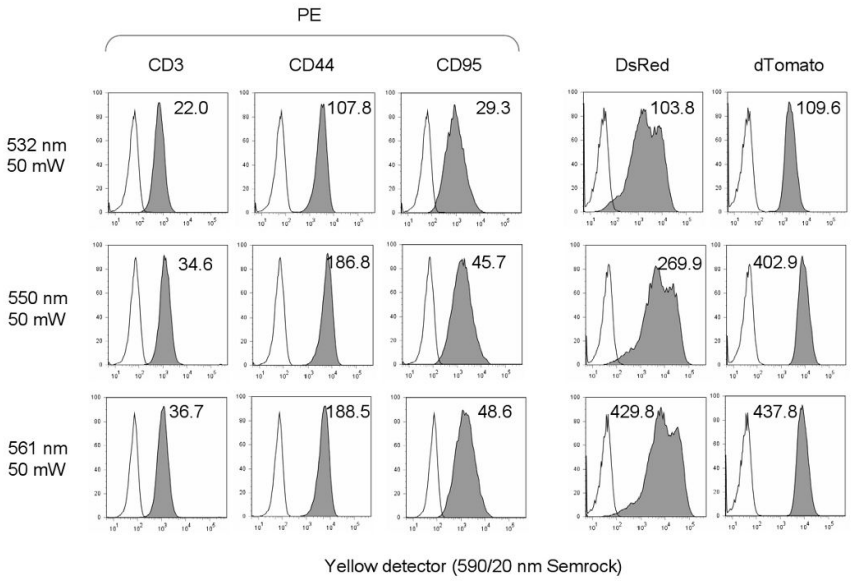

Figure 3. PE and red fluorescent proteins

Three left columns, EL4 mouse thymoma cells were labeled with biotin-anti-CD3, CD44 or CD95 antibody followed by streptavidin conjugated to PE, and analyzed on the LSR II™ using 532, 550 or 561 nm lasers at matched power levels and the same optical detection path. *Two right columns*, SP2/0 cells were stably transfected with DsRed and dTomato and similarly analyzed. All cells were analyzed through a 590/20 nm bandpass filter (to accommodate the 561 nm laser). Filled peaks indicate labeled cells, unfilled peaks indicated unlabeled controls. The sensitivity indices (described in the Materials and Methods) are indicated on each histogram. PMT voltages were fixed for all samples.

NIH-PA Author Manuscript

NIH-PA Author Manuscript

NIH-PA Author Manuscript

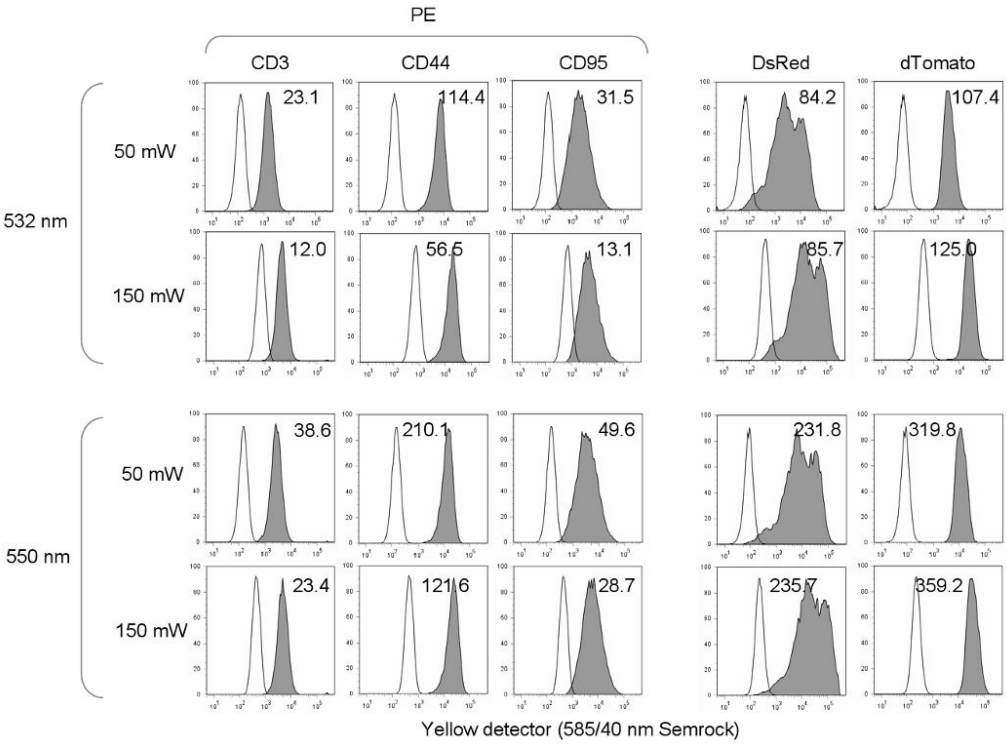

Figure 4. PE and red fluorescent proteins at higher power levels

Three left columns, EL4 mouse thymoma cells were labeled with biotin-anti-CD3, CD44 or CD95 antibody followed by streptavidin conjugated to PE, and analyzed on the LSR II using 532 nm lasers at 50 and 150 mW, and the 550 nm laser at 50 and 150 mW. *Two right columns*, SP2/0 cells were stably transfected with DsRed and dTomato and similarly analyzed. All cells were analyzed through a 585/40 nm bandpass filter. Filled peaks indicate labeled cells, unfilled peaks indicated unlabeled controls. The sensitivity indices (described in the Materials and Methods) are indicated on each histogram. PMT voltages were fixed for all samples.

NIH-PA Author Manuscript

NIH-PA Author Manuscript

NIH-PA Author Manuscript

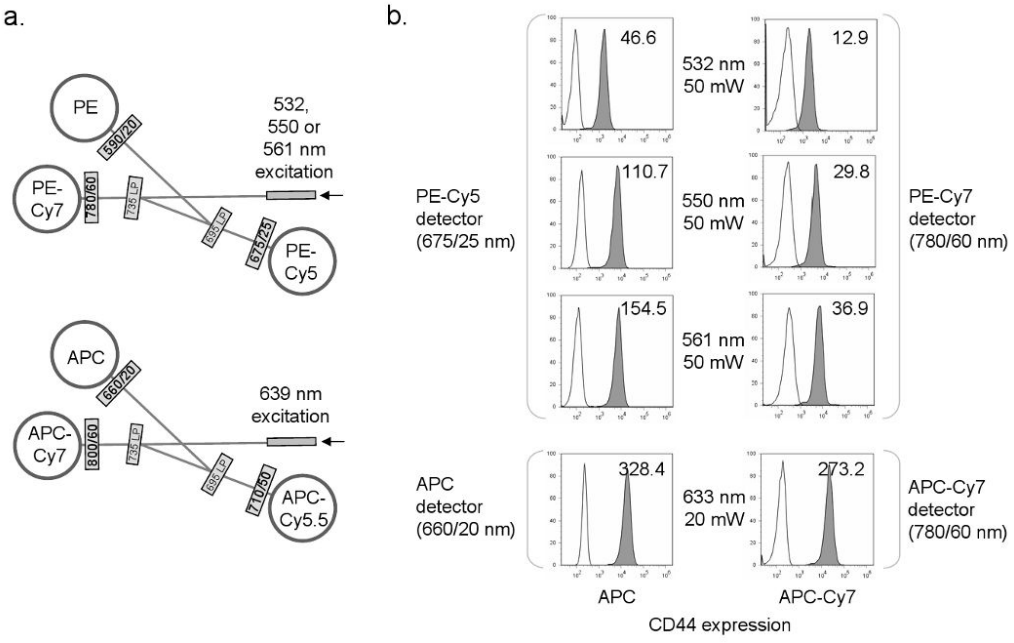

Figure 5. APC excitation by green-yellow lasers

a, optical configuration for the BD LSR II™, with APC, APC-Cy5.5 and APC-Cy7 detected in one trigon using a red diode laser (639 nm), and PE, PE-Cy5 and PE-Cy7 detected through a separate trigon using either 532, 550 or 561 nm excitation. ***b***, EL4 cells labeled with APC- or APC-Cy7 conjugated anti-CD44 (left and right columns respectively) were analyzed with 532, 550 or 561 nm laser light and detected through a 675/20 nm PE-Cy5 or 780/60 nm PE-Cy7 filter (top three histograms). The same cells were also analyzed with HeNe 633 nm laser light and detected through a standard 660/20 nm APC filter (bottom histograms).

NIH-PA Author Manuscript

NIH-PA Author Manuscript

NIH-PA Author Manuscript

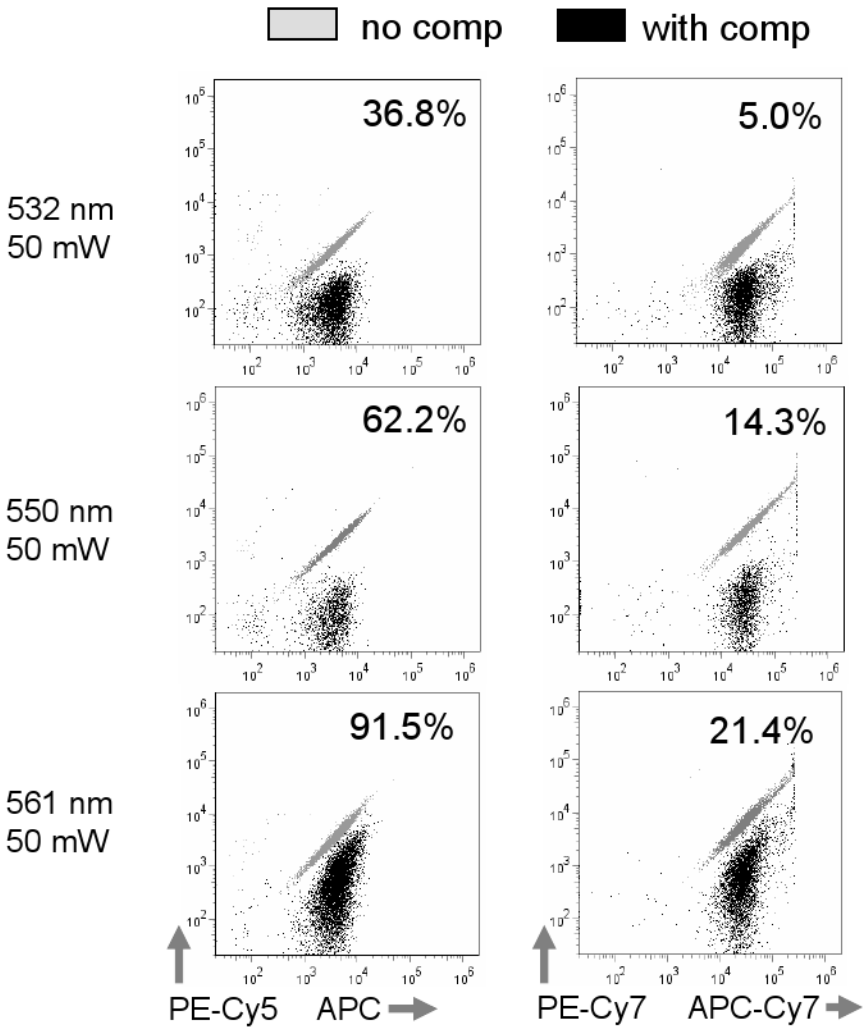

Figure 6. Spectral overlap from green-yellow laser excitation

Analysis of APC and APC-Cy7 labeled cells using the filter/detector configuration shown in Figure 8. APC and APC-Cy7 signal overlap into the PE-Cy5 and PE-Cy7 detectors is shown in overlaid dotplots without and with computer-calculated compensation (grey and black dots, respectively). Values for PE-Cy5 -% APC or PE-Cy7 - %APC-Cy7 fluorescence are shown on each plot.

NIH-PA Author Manuscript
NIH-PA Author Manuscript
NIH-PA Author Manuscript

Table 1

Fluorescent microspheres

The indicated fluorescent microspheres were used in this study, and are referenced in the text.

Microspheres	Manufacturer	Catalog No.	Dye	Population number	MESF value(s)
Rainbow Premixed	Spherotech	RCP-30-5A	Proprietary	7 (plus one null)	N/A
MESF FITC	Bangs/Polysciences	BLI824B-5	Fluorescein	4 (plus one null)	2638
					7800
					22810
					70751
MESF PE	Bangs/Polysciences	BLI827B-5	R-PE	4 (plus one null)	2233
					8836
					77090
					351120

NIH-PA Author Manuscript NIH-PA Author Manuscript NIH-PA Author Manuscript

Table 2

PE and red fluorescent proteins on a jet-in-air cell sorter

Sensitivity index values are shown for BD FACSVantage DiVa™ analysis EL4 mouse thymoma cells were labeled with biotin-anti-CD3, CD44 or CD95 antibody followed by streptavidin conjugated to PE, and SP2/0 cells were stably transfected with DsRed and dTomato. Cells were analyzed on a using a 532 nm laser at 150 mW, and the 550 nm laser at 50, 100 and 150 mW. All cells were analyzed through the same 585/40 nm bandpass filter shown in Figure 4. PMT voltages were fixed for all samples.

		Sensitivity indices				
		EL4 cells labeled with PE-conjugated			SP2/0 cells expressing	
Laser wavelength (nm)	**Laser power (mW)**	**CD3**	**CD44**	**CD90**	**DsRed**	**dTomato**
550 nm	50	12.4	108.5	18.6	45.2	102.8
	100	12.2	102.7	17.1	59.0	133.5
	150	10.2	80.6	12.7	63.6	143.1
532 nm	150	9.87	82.7	15.1	27.6	58.5